LAWRENCE
LIVERMORE
NATIONAL
LABORATORY

LLNL-TR-400902

Stable Spheromaks with Profile Control

T. K. Fowler, R. Jayakumar

January 31, 2008

Disclaimer

This work performed under the auspices of the U.S. Department of Energy by Lawrence Livermore National Laboratory under Contract DE-AC52-07NA27344.

Stable Spheromaks with Profile Control

T. K. Fowler* and R. Jayakumar

Lawrence Livermore National Laboratory

Abstract

A spheromak equilibrium with zero edge current is shown to be stable to both ideal MHD and tearing modes that normally produce Taylor relaxation in gun-injected spheromaks. This stable equilibrium differs from the stable Taylor state in that the current density j falls to zero at the wall. Estimates indicate that this current profile could be sustained by non-inductive current drive at acceptable power levels. Stability is determined using the NIMROD code for linear stability analysis. Non-linear NIMROD calculations with non-inductive current drive could point the way to improved fusion reactors.

1. Introduction

Spheromaks achieve toroidal-like plasma confinement, as in tokamaks, but without the toroidal field coils that define the size and cost of tokamaks. Building on earlier results in CTX [1], remarkably stable spheromak equilibria confining plasmas at electron temperatures up to 500 eV and peak electron $\beta \approx 10$ % have now been achieved in the SSPX experiment using helicity injection by electrostatic guns to create a plasma that then heats up as magnetic fluctuations die away during the slow decay of the current [2]. Due to magnetic relaxation, gun injection tends to produce a current density **j** and magnetic field strength B such that $\lambda = \mu_o(j_{||}/B)$ is roughly constant on closed flux surfaces, giving high resistive losses near the edge. Despite these losses, attractive steady state spheromak fusion reactors were thought to be possible for gun efficiencies ideally achievable [3]. Thus far, the required efficiencies have not been achieved in steady state, because of continuing magnetic turbulence as long as gun injection is required to sustain the plasma [4].

*Consultant. E-mail: Fowler @ nuc.berkeley.edu

Here we discuss an alternative approach based on newly discovered equilibria that are stable to the ideal MHD and tearing modes typically encountered with gun injection, even though for this state λ falls to zero at the walls with zero gun current and small resistive losses at the edge of the plasma. As with the familiar Taylor state with constant λ [5], stability requires flattening the λ profile, but only in the interior. This is not a natural state in the absence of instability, due to non-uniform resistivity that tends to create gradients in λ. However, such a profile could be sustained in steady state using neutral beams or other non-inductive current drive, with acceptable power requirements according to estimates presented here as motivation for future work.

The main focus of this paper is linear stability against tearing modes. The stable equilibrium is discussed in Section 2. Stability calculations using the NIMROD code [6] are presented in Section 3. Estimates of current drive power required to maintain a stable state are presented in Section 4. Results are summarized in Section 5, with suggestions for future work on NIMROD to extend our work to the non-linear regime.

2. Stable Equilibria with Zero Edge Current

The flux averaged <j> for the Taylor state with constant λ, shown in Fig. 1, is dominated by a strong toroidal current near the magnetic axis and poloidal current about half this strength near the boundary. Thus, though the Taylor state is stable to tearing, <j> extends to the edge where temperatures are low and the power required to drive j is large.

To seek stable equilibria with smaller edge losses, we take:

$$\lambda(\psi) \quad = \quad \lambda_o[1 - (\psi/\psi_E)^N] \quad , \qquad \lambda = 0 \text{ for } 0 < \psi < \psi_E \qquad (1)$$

where ψ is the poloidal magnetic flux function with $\psi = \psi_E$ at the plasma edge. The Grad-Shafranov equilibrium equation is solved using the Corsica code with SSPX flux conserver geometry including an electrostatic gun with poloidal field coils producing a bias flux ψ_E on open field lines [7, 8]. Here the gun voltage generating current in SSPX is set equal to zero, represented in Eq. (1) by $\lambda = 0$ for $0 < \psi < \psi_E$ (taken positive), while j inside closed surfaces is assumed to be maintained by neutral beams or other non-

inductive current drive. As is discussed in Ref. [7], the actual inputs to Corsica are the plasma pressure $p(\psi)$ and $F(\psi) = RB_\phi$, taken as $dF/d\psi = \lambda(\psi) \rightarrow (\mu \mathbf{j}\cdot\mathbf{B}/B^2)$ at $p = 0$, and the total toroidal current relative to the bias flux that fixes λ_o. In Corsica, the hoop force is confined by toroidal image currents in the flux conserver wall, whereas in steady state additional poloidal field coils would be required. No toroidal field coils are required.

The shape of the current profile is controlled by N in Eq. (1). An example equilibrium for N = 6 is shown in Fig. 2 giving profiles for λ, j, q and the nominal small pressure p included in the calculation. Fig. 3 displays the closed flux surfaces where $\lambda \neq 0$. For numerical convenience, the quantities plotted in Figs. 1 and 2 are defined by:

$$\langle\lambda\rangle = \mu_o(\langle \mathbf{j}\cdot\mathbf{B}\rangle/\langle B^2\rangle) \qquad (2)$$

$$\langle j\rangle = (\langle \mathbf{j}\cdot\mathbf{B}\rangle/\langle B^2\rangle^{1/2}) \qquad (3)$$

Note the flattened λ profile in Fig. 2. In Section 3, we will show that this state is stable to tearing, even though the current falls to zero at the edge, with interesting consequences for fusion energy applications, as discussed in Sections 4 and 5.

3. Stability Analysis

In SSPX, Taylor relaxation leads to a quasi-stable state with a relatively flat λ profile inside closed flux surfaces, but with a larger value of λ representing gun current on open field lines during helicity injection. Typically instabilities feeding helicity into the closed region are dominated by n = 1 kink modes due to this gun current. Tearing instability opens field lines in 3D, even when the 2D projection has the closed surfaces predicted by Taylor relaxation. It has been shown that allowing the gun current to fall below the threshold for instability causes flux closure in 3D, evidenced by high electron temperatures in SSPX [2]. This suggests that equilibria given by Eq. (1), which have no current on open field lines, might be sufficiently stable if also there are no internal modes inside the last closed surface (the separatrix) and if known ideal MHD tilt and shift external modes are stabilized. Stability of the equilibrium in Figure 2 to tilt and shift modes (n = 1) has been verified using the DCON code [9]. The tilt mode is stabilized by

the conducting wall of the flux conserver. In a steady state device, stabilizing the tilt mode would require active feedback, probably feasible.

Verifying stability against tearing modes that can destroy flux surfaces requires further analysis. The straightforward approach involves calculating the free energy parameter Δ' which usually requires numerical computation. The existence of states with zero edge current that are stable to tearing and kink modes at zero pressure was suggested by Robinson's earlier calculations of Δ' for a linear diffuse pinch as a model of RFP's [10]. Here we demonstrate linear stability for similar states in a spheromak, using NIMROD.

The reader may ask, if theory predicts tearing-stable profiles, why both RFP's and spheromak experiments have exhibited tearing of flux surfaces detrimental to good confinement. The main reason, as noted in the Introduction, is that stability requires flattening the λ profile in the interior, an unnatural state in the absence of instability due to non-uniform resistivity that tends to create gradients in λ. Hence profile control is required, as discussed in Sections 4 and 5 and now demonstrated in RFP experiments [11].

A. Stability versus N: Analytical, Straight Cylinder Model

That flattening the λ profile in the plasma interior is the key to stability against tearing was shown by Robinson's calculations of Δ' for the cylinder model of RFP's, with several examples [10]. Before proceeding with the discussion of our NIMROD results, we first discuss a well-known analytical approximation for Δ' in tokamaks giving a stability parameter $\propto (rj_{||}\,'/B_\theta)$ [12]. Multiplying and dividing by B_z (constant for tokamaks) gives $\mu_o(rj_{||}\,'/B_\theta) \rightarrow aq\lambda'$ for spheromaks and RFP's with safety factor $q = (rB_z/aB_\theta)$ for major radius a, giving in turn the following approximate criterion for stability [12]:

$$\left|(qr\mu_o/q'B_\theta)(d(\mathbf{j}\cdot\mathbf{B}/B_z)/dr)\right| \quad \rightarrow \quad \left|aq^2(\lambda'/q')\right| \quad < \quad m \qquad (4)$$

where (λ'/q') with $' \equiv d/dr$ is the important factor in the destabilizing term of the free energy $\delta W \propto -r\Delta'$. Here all quantities are to be evaluated at a magnetic resonance $q =$

m/n with poloidal mode number m and toroidal number $n = k_z a$ for circularized flux surfaces equivalent to the cylinder model which, for spheromaks, has radius $a = R/2$ with flux conserver radius R and length $L = 2\pi a$.

According to Eq. (4), in the interior the stability of flattened λ profiles follows from the weaker gradient in λ versus q, evident in the stable profile of Fig. 2, while stability at the edge is aided by the fact that $q \rightarrow 0$ there. The crucial region lies between, requiring more careful examination of λ in Eq. (1) versus q, given for the cylinder model by (with $\psi = r^2/a^2$ for the cylinder):

$$\lambda a \quad = \quad \lambda_o a[1 - (r^2/a^2)^N] \quad = \quad [2q - r(dq/dr)]/[q^2 + (r^2/a^2)] \qquad (5)$$

Near the magnetic axis, we expand $q = q_o[1 - A(r/q_o a)^2 + \cdots]$ and substitute this into Eq. (6) giving to lowest order $q_o = 2/(\lambda_o a)$ and A and the relationship. Using also the fact that the volume average $\langle\lambda\rangle = \lambda_o N/(N + 1) \approx 2/a$, the Taylor state value, we obtain $\lambda_o = (2/a)(N + 1)/N$ and $q_o = N/(N + 1)$. This q profile gives instability at $r = 0$ for $N = 1$ but stability for $N \geq 2$. To explore the edge, we can set $q = 0$ in the numerator and denominator in Eq. (5) giving $dq/dx = 1/2\ \lambda a$ with $x = r^2/a^2$. This too gives stability for $N \geq 2$, marginally so for resonances around $r/a \approx 0.5$ where the corresponding $|\Delta' a|$ is smallest.

Though qualitatively in agreement with Robinson's findings, these analytical results do not yield accurate thresholds for stability. Pearlstein has calculated Δ' for a cylinder model with aspect ratio and boundary conditions appropriate for spheromaks, and finds the stability threshold to be $N > 5$ for λ profiles in the cylinder approximating those in Eq. (1) [13]. Also, toroidal effects are very important for spheromaks.

Quantitative guidance requires further numerical computation, to which we now turn, using NIMROD that also takes account of toroidal effects.

B. Numerical Stability Analyses Using NIMROD

NIMROD is a non-linear resistive MHD code evolving initial states in time in 3D [6]. Here we use this code only to verify the linear stability of the equilibria described in Section 2, including toroidal effects, as follows.

The 2D equilibria calculated using the Corsica code, discussed in Section 2, are accurately introduced into the NIMROD code. Then linear stability (of both ideal MHD and tearing modes) is tested by time dependent calculations with non-linear terms disabled, to determine if initial perturbations grow in time. For numerical convenience we restrict attention to internal modes, in that a toroidally-closed conducting wall is introduced at the last closed flux surface shown in Fig. 3. This test is carried out for values of N = 2 to 6 in Eq. (1) in order to detect numerically the threshold value of N above which stability is obtained. Modes with toroidal mode numbers n up to 10 were investigated.

Fig. 4 shows the λ and q profiles for N = 2, 3 and 4 (see Figure 2 for N = 6 profiles). In NIMROD calculations, the modes with toroidal mode numbers n = 4 and n = 5 had positive growth rate for N = 2 and the growth rate of the perturbation energy is shown in Fig. 5. (Note that the N = 2 case does not have a q = 1/3 surface to support a n = 3 mode). For N = 3, the n = 3 mode is unstable and the linear growth rate is also shown in Figure 5. In contrast to these cases, for N = 4, all modes are observed to be stable. This is illustrated in Fig. 6 by the negative growth rate for n = 3, 4 and 5. Other mode numbers also give negative growth rate for N = 4. These calculations were repeated for N = 5 and N = 6 and these also show stability to all modes up to n = 10.

Therefore NIMROD confirms our expectation that sufficiently flat λ profiles are stable to current-driven ideal and resistive internal modes. For the equilibrium model of Eq. (1), the threshold value for stability as indicated by NIMROD is $3 \leq N \leq 4$, indicating less flattening to achieve stability than did the cylinder model, presumably due to the toroidal effects included in NIMROD.

4. Current Drive Power

To assess the relevance of our work to fusion energy research, we calculate the power P_{CD} required to sustain the current for the stable equilibrium in Figure 2, and then calculate as a figure of merit the fusion power gain Q given by:

$$Q = P_F/P_{CD} = (4\pi R^2/0.8)(P_W/P_{CD}) \qquad (6)$$

$$P_W = (0.8/4\pi R^2)\int dV(1/4\ n^2\sigma v\ 17.6\ MeV) = 0.11 n_o^2 R\ \sigma v_o\ C_F \qquad (7)$$

In Eq. (6), P_F is the fusion power (80% neutrons), expressed on the right in terms of the power density P_W of fusion neutrons bombarding a spherical vacuum chamber of radius R that also serves as a flux conserver. In Eq. (7) defining P_W in MW, n in units $10^{20}\ m^{-3}$ and σv in units 10^{-22} have values at the magnetic axis (denoted by subscript o), weighted by $C_F = \int dV/V\ (n/n_o)^2(\sigma v/\sigma v_o)$. In calculating the numerical factor 0.11, we approximate the plasma volume as a cylinder giving $V = 2\pi^2 a^3$ with a = R/2 as in Section 3.

For concreteness, in calculating P_{CD} we focus on neutral beam current drive. The current generated by neutral beams in spheromaks is given in Ref. [14] using Monte Carlo calculations for the slowing down of beam ions by collisions with electrons and plasma ions. A good representation of such calculations is [15]:

$$j = e(S\tau)\underline{v}\ (1 - 1/Z_{Eff})\cos\theta \propto (SE)(TJ/n) \qquad (8)$$

with beam injection at an angle θ relative to field lines; beam deposition rate S per unit volume; beam ion slowing down time by electron collisions $\tau \propto T^{3/2}/n$; a screening factor due to electron current containing Z_{Eff} ; and a mean ion speed $\underline{v} \propto (E/T^{1/2})J$ with beam energy E and a factor J discussed below. On the right, we assume a fixed value for Z_{Eff} (≈ 2) and for θ (= 0, parallel injection). Solving Eq. (8) for the deposition power density SE gives, with $j \propto I$ (the total current) and numerical factors obtained from Ref. [15]:

$$P_{CD} = \int dV\ SE = 20\ (In_oR/T_o)C \qquad (9)$$

$$C = 0.18\int dV/V\ (n/n_o)(j/j_o)[(7/X_o^2) + X_o(T_o/T)^{3/2} + 2(T_o/T)] \qquad (10)$$

Here power is in MW for current in MA, with T in KeV. The integrand in weighting factor C is obtained using, from Ref. [13], $J = X^2/[(7 + X^{3/2} + 2X^2]$ with $X^2 = (E/15T)$ for deuterium beams, the factor 0.18 being the maximum value of J for any X. For the current profile of Figure 2 and $T = T_o(1 - 0.99\psi)$ in a reactor (100 eV edge

temperature), C = 0.5 for a density profile $n \propto T$ for the optimum $X_o = 1.5$, but C = 2 for constant n. Thus reactor optimization may require pellet fueling to cause n to peak at the center, except at the edge where the beam provides most of the density just to carry the current ($n \propto j$). Assuming $n \propto j$ everywhere gives C = 0.8.

Eq. (9) exhibits the scaling for current drive power in Ref. [16] and it fits numerically results for parallel injection into a spheromak in Ref. [14]. It also fits results in Ref. [17] for the DIIID tokamak when corrected to take into account tokamak geometry (spheromak R twice the tokamak major radius), limited beam access due to the toroidal coils (giving $\theta \approx 70^o$) and a factor 2 degradation due to instability driven by super-Alfvenic ion wave excitation in these experiments [17].

Eqs. (6) - (10) can be used to explore the reactor potential for a spheromak employing neutral beams to maintain a stable current profile. The reactor size to achieve a given Q and wall load can be found as follows. First we solve Eq. (7) for n in terms of the wall load. For T_o = 50 KeV (chosen to reduce electron drag on beam ions), we obtain, with $\sigma v = 8.7$, $n = 1.0 (P_W/C_F R)^{1/2}$. Then we introduce this n into Eq. (6), having first obtained Q in terms of n by substituting Eqs. (7) and (9) into Eq. (6), and we solve the resulting equation for R, giving:

$$R = 0.089\, P_W^{-1/3} (IQ)^{2/3} (C^2/C_F)^{1/3} = 0.089\, P_W^{-1/3} (IQ)^{2/3} \qquad (11)$$

where on the right we have set the weighting factor $(C^2/C_F))^{1/3} = 1$ for a peaked density profile (C = 0.5, $C_F \approx 0.33$). At fixed Q, both the fusion power and the beam power scale as $R^2 P_W \propto P_W^{1/3}$ giving a fixed cost per kW of fusion power for beams but a lower confinement facility cost per kW at higher P_W.

Guessing I = 50 MA for ignition (the value in Ref. [3]), Q = 20 gives R = 3 m for $P_W = 20$ MW/m^2 (the parameters of Ref. [3]) and R = 5 m for $P_W = 5$ MW/m^2 as in most reactor studies. This is to be compared with an equivalent R = 20 m for ITER and R = 10 m for the ARIES-AT advanced tokamak reactor [18]. The required beam power is $P_{CD} \approx 100$ MW with $E \approx 1$ MeV , in the range of the beam system for ITER. Higher wall loads and smaller size are achievable with "liquid walls," especially for pulsed reactors [19].

5. Discussion

The potentially small size of spheromak reactors discussed in the previous section, with no toroidal coils, continues to offer an attractive alternative route to fusion power, if the good plasma confinement exhibited in SSPX extrapolates to larger systems. The main difficulty concerns steady state operation, not yet achieved with good confinement during steady state sustainment by gun injection, perhaps for fundamental reasons [20]. Sustaining the current by neutral beams or other non-inductive current drive appears to be a viable alternative, in which the current drive system also exercises profile control to maintain a stable state of the kind discussed in Sections 2 and 3.

The confidence to pursue a spheromak program with current drive could be greatly strengthened by more computer simulations, using the NIMROD code already validated extensively to explain magnetic turbulence in SSPX and the conditions required to achieve low turbulence levels and good energy confinement [4]. A similar effort has already led to successful profile control and record temperatures in the MST reversed field pinch [11]. A concerted effort using NIMROD could address many open issues, about physics, suitable experiments and reactor prospects.

An important physics issue concerns effects at finite β. Experiments in SSPX have already achieved $\beta \approx 10\%$, comparable to that in the reactor design of Ref. [3], but transiently, during plasma decay on the L/R timescale $\tau = (\mu_o/2\eta\lambda^2)$ with resistivity η [2]. For steady state, theory has long predicted the slow growth of magnetic islands on about this timescale for plasmas with finite β and negative shear ($q'/q < 0$) as in spheromaks, even if tearing modes are stabilized ($\Delta' < 0$), at a rate given approximately by [21]:

$$d(w/a)^2/dt = (1/\tau)[- (w/a)|\Delta' a| + \beta G] \qquad (12)$$

Here w is the island width and G is a geometric factor proportional to $|p'/p|$ and magnetic scalelengths. The most vulnerable zone is probably midway between the magnetic axis

and the edge where β is still large and $|\Delta' a|$ is smallest for the stabilized current profile, as discussed in Section 3A, giving a saturated width $w/a = (\beta G/|\Delta' a|)$. The NIMROD simulations advocated here could explore pressure-driven resistive instabilities and their non-linear consequences, with more attention to gridding around resonances in steady state than has yet been attempted in our work or in SSPX analysis. Otherwise, the main physics issue appears to be achieving a λ profile sufficiently flat in the interior. Given a profile stable to ideal and resistive MHD modes, we might expect tokamak-like energy confinement, and indeed confinement in SSPX can be shown to be no worse than L-mode scaling, while the $n\tau$ assumed in Ref. [3] is comparable to ITER-98P(y,2) scaling.

While experimental design and reactor studies are outside the scope of this paper, preliminary ideas are discussed in Ref. [22]. Briefly, experiments with neutral beams should anticipate the need to control the λ profile during buildup: without profile control, inductive drive alone does not yield a fully stable state in RFP's and stably decaying spheromaks eventually evolve toward strongly unstable states. That said, it may be best to build up current using the neutral beams to maintain profile control during buildup, or perhaps a combination of beams and flux control [23]. Buildup could be initiated on a gun-created target plasma, as in SSPX, with a target magnetic field strength just adequate to confine beam ions and to assure that ion speeds are sub-Alfvenic (to avoid TAE modes).

Estimates yielding a representative series of experiments employing neutral beam buildup are given in Ref. [22]. Preliminary calculations using the code employed in Ref. [24] confirm the possibility of driving all of the current using an array of neutral beams aimed so as to produce a desired λ profile. Quantitative results could be obtained by installing on NIMROD one of the neutral beam packages now used in tokamak codes to calculate the beam power more accurately, giving also a means for optimizing the number of beams and their injection angles to achieve a stable state while simultaneously monitoring the quality of flux surfaces. Our studies suggest considerable latitude in stable profile shapes, so long as the λ profile is flatter in the interior than would normally be the case without profile control. Unlike small tokamaks, spheromaks have beam access to achieve optimal aiming nearly parallel to field lines ($\cos\theta \approx 1$), requirements being similar to those explored in mirror devices including the Field Reversed Mirror with coil

geometry and goals similar to the spheromak discussed here [25]. The main cost for an experimental program to pursue these ideas could be avoided by sharing existing neutral beam systems employed in tokamak research [22]. For reactors, the beam power would generally be higher in spheromaks which have zero bootstrap current, compared to ARIES-AT that assumes 91% bootstrap current [18]. But NIMROD studies could provide the physics input for an ARIES-like spheromak study to elucidate tradeoffs between higher injection power versus the lower cost and much simpler divertor of spheromak confinement systems [22].

In summary, we have shown the existence of states linearly stable to tearing and ideal MHD modes in spheromaks, with no need to achieve stability by the toroidal field coils that have characterized tokamaks and determined the pace and cost of research leading to ITER. Historically, it was the ideal and resistive MHD physics featured in NIMROD that drove research toward the tokamak solution. NIMROD simulations extending our work could help decide whether the toroidal field coils of tokamaks are really necessary, perhaps paving the way to better fusion reactors in the future, in parallel with ITER.

Acknowledgements

The authors wish to thank D. Brennan, B. I. Cohen, E. B. Hooper, L. L. Lodestro and C. R. Sovinec for many helpful discussions. We especially thank L. D. Pearlstein for his unpublished calculations of Δ' for a cylinder approximation of a spheromak that helped motivate this work. This work was supported in part by the U. S. Department of Energy under contracts W7405-ENG-48 and DEAC 52-07NA27344 at the Lawrence Livermore National Laboratory.

References:

[1] F. J. Wysocki, J. C. Fernandez, I. Hennins, T. R. Jarboe and G. J. Marklin, Phys. Rev. Letters **61**, 2457 (1988).

[2] H. S. McLean, R. D. Wood, B. I. Cohen, E. B. Hooper, D. N. Hill, J. M. Moeller, C. Romero-Talamas, and S. Woodruff, Phys. Plas. **13**, 0556105 (2006). This paper reports T = 350 eV; T = 500 eV is reported in a subsequent paper submitted for publication.

[3] R. L. Hagenson and R. A. Krakowski, Fus. Tech. **8**, 16011 (1985).

[4] B. I. Cohen, E. B. Hooper, R. H. Cohen, D. N. Hill, H. S. McLean, R. D. Wood and S. Woodruff, Phys. Plas. **12**, 056106 (2005).

[5] J. B. Taylor, Rev. Mod. Phys. **58**, 741 (1986).

[6] C. R. Sovinec, T. A. Gianakon, E. D. Held, S. E. Kruger and D. D. Schnack, Phys. Plasmas **10**, 1727 (2003).

[7] E. B. Hooper, L. D. Pearlstein and R. H. Bulmer, Nucl. Fus. **39**, 863 (1999).

[8] L. D. Pearlstein, R. H. Bulmer, T. A. Casper, E. B. Hooper, R. A. Jong, T. B, Kaiser. L. L. Lodestro and H. L. Berk, 28 th European Physical Society Conference on Controlled Fusion and Plasma Physics, Madeira, Portugal, 2001.

[9] A. H. Glasser and M. S. Chance, "Determination of Free Boundary Ideal MHD Stability with DCON and VACUUM," Bull. Am. Phys. Soc. **42**, 1848 (1997) https://fusion.gat.com/THEORY/dcon/

[10] D. R. Robinson, Nucl. Fus. **18**, 939 (1978).

[11] D. J. Den Hartog, et al., Nucl. Fus. **47**, L17 (2007). This paper reports T = 1.3 KeV achieved by profile control; T = 2 KeV will be reported in a paper in progress (S. C. Prager, private communication).

[12] C. C. Hegna and J. D. Callen, Phys. Plas. 2308 (1994).

[13] L. D. Pearlstein, private communication.

[14] A. F. Lifschitz, R. Farengo and N. R. Arista, Plas. Phys. Controlled Fus. **44**, 1979 (2002).

[15] D. R. Mikkelsen and C. E. Singer, Nucl. Tech./Fusion **4**, 237 (1983).

[16] J. G. Cordey, Plas. Phys. Controlled Fus. **26**, 123 (1984).

[17] M. Murakami et al., Phys. Plas. **13**, 056106 (2006).

[18] F. Najmabadi et al., Fus. Eng. Design **80**, 3 (2006).

[19] T. K. Fowler, D. D. Hua, E. B. Hooper, R. W. Moir and L. D. Pearlstein, Comments on Plas. Phys. Controlled Fus./Comm. Mod. Phys. C **1**, 83 (1999).

[20] T. K. Fowler and R. Gatto, Plas. Phys. Controlled Fus. **49**, 1673 (2007).

[21] M. Kotshenreuther, R. D. Hazeltine and P. J. Morrison, Phys. Fluids **28**, 294 (1985).

[22] T. K. Fowler, "A Development Path for the Stabilized Spheromak Reator," UCRL-TR-232757 July 16, 2007.

[23] E. B. Hooper, D. N. Hill, H. S. McLean, C. A. Romero-Talamas and R. D. Wood, Nucl. Fusion **47**, 1064 (2007).
[24] L. D. Pearlstein, T. A. Casper, D. N. Hill, L. L. Lodestro and H. S. McLean, "A Calculation of Neutral Beam Injection in SSPX.\," 33 rd European Physical Society Conference on Controlled Fusion and Plasma Physics, Rome, ECA**301**, 5 (2006).
[25] T. K. Fowler, "Mirror Theory," *Fusion*, E. Teller, Ed., Academic Press, New York, 1981, Chap. 5, Volume 1A.

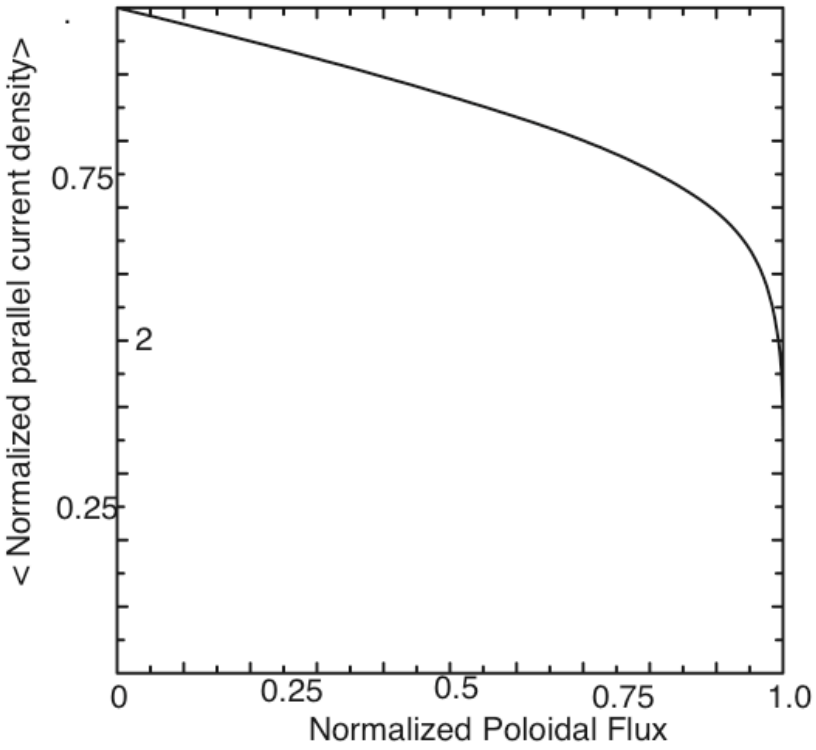

Fig.1 Flux surface averaged parallel current density vs normalized poloidal flux for Taylor state.

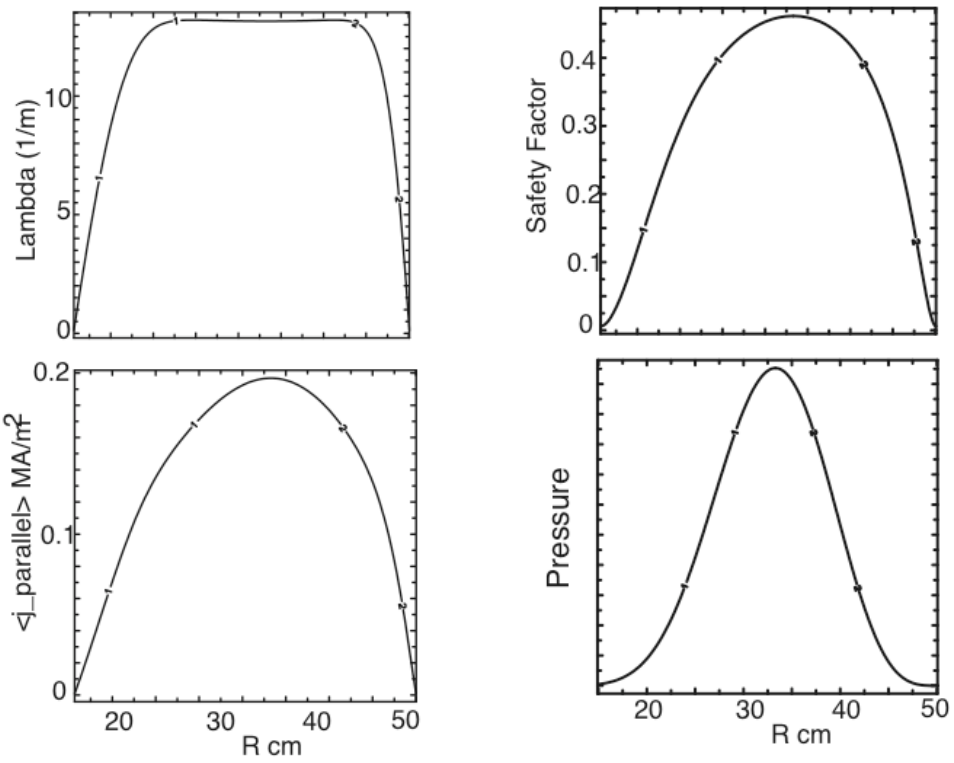

Fig. 2 Profiles for exponent N=6 (Eq. (1))

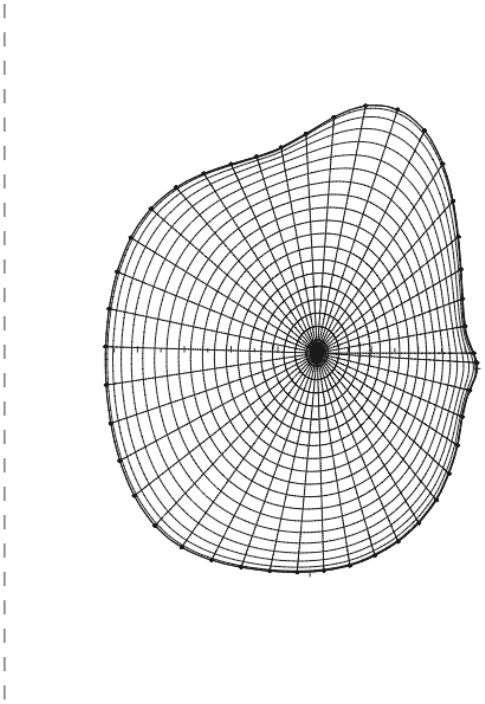

Fig. 3 Poloidal flux contours for profile shown in Fig. 2 (N=6)

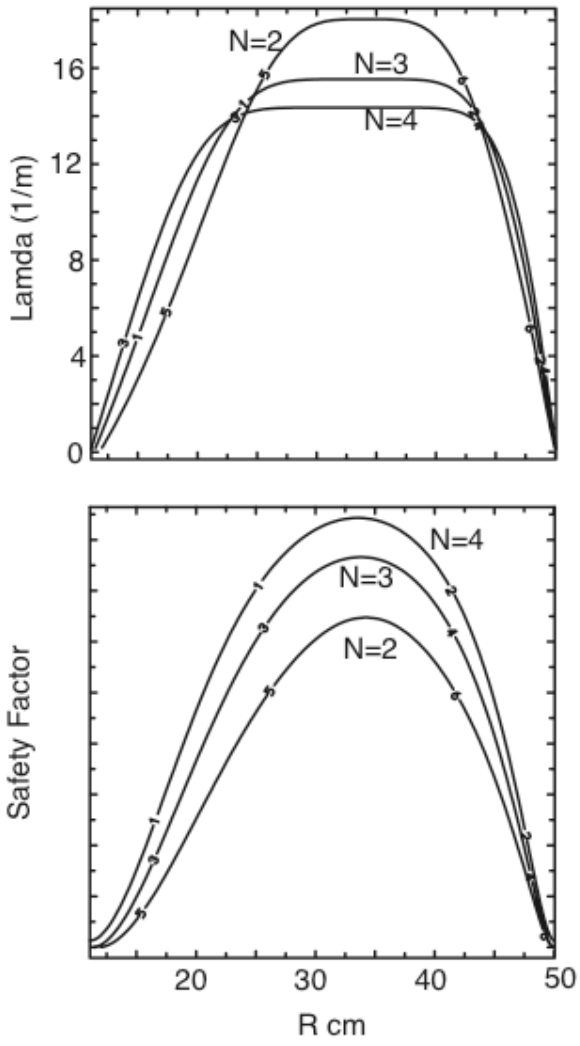

Fig.4 λ and q profiles for N=2,3 and 4; for N=2 the maximum value of q is 0.321.

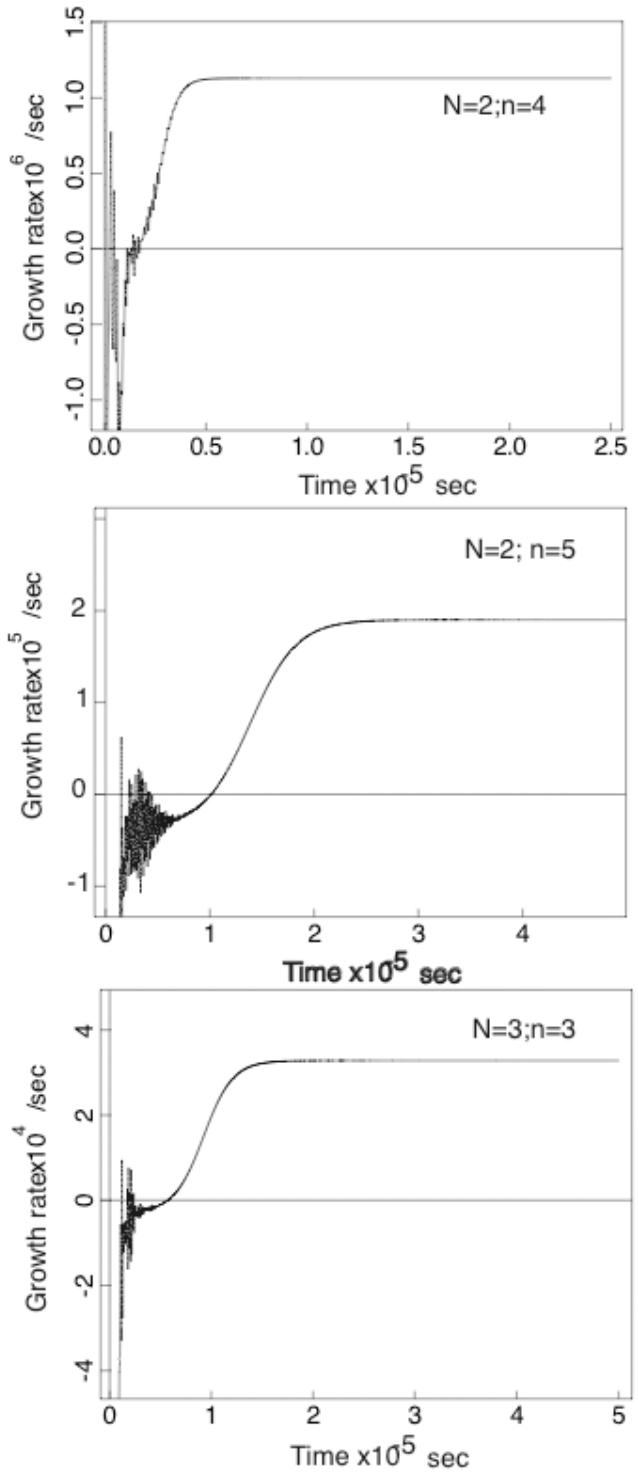

Fig.5 The growth rate results from NIMROD for N=2 and 3 showing instabilities. Constancy of growth rate shows convergence of the time dependent calculations.

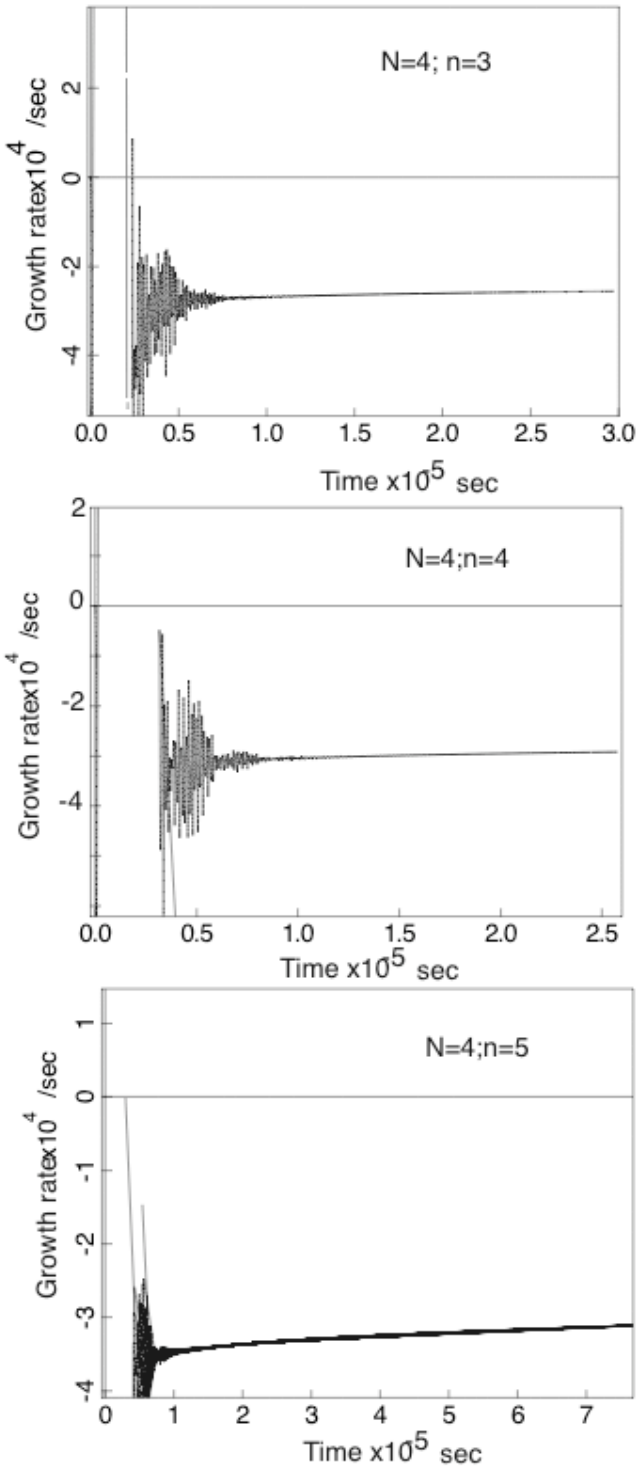

Fig.6 Growth rate (negative) for a few of the toroidal mode numbers for N=4 indicating stability.